Microscopic Analysis of the Different Perchlorate Anions Intercalation Stages of Graphite

R. Yivlialin[1], G. Bussetti[1], L. Brambilla[2], C. Castiglioni[2], M. Tommasini[2], L. Duò[1], M. Passoni[3], M. Ghidelli[3], C. S. Casari[3], A. Li Bassi[3]*

[1] *Deaprtment of Physics, Politecnico di Milano, p.za Leonardo da Vinci 32, I-20133 Milano (Italy).*

[2] *Deaprtment of Chemistry, Materials and Chemical Engineering, Politecnico di Milano, p.za Leonardo da Vinci 32, I-20133 Milano (Italy).*

[3] *Department of Energy, Politecnico di Milano, via Ponzio 34/3, I-20133 Milano (Italy).*

*) corresponding author: gianlorenzo.bussetti@polimi.it

ABSTRACT. Driven by the perspective of large-scale, high-quality graphene production via chemical routes, the investigation of electrochemical anion intercalation between the basal graphite planes has seen a renewed interest among the scientific community. At relatively high electrochemical potentials, when oxidation occurs, graphite electrodes undergo significant anion intercalation processes. The latter swell the uppermost graphite layers (*i.e.* graphene sheets),

reduce the inter-plane interaction and favor the graphite delamination in liquid. Different intercalation stages are observed in a perchloric acid electrolyte, which are usually interpreted in terms of different perchlorate penetration depths. Nonetheless, the understanding of the morphological changes occurring at the electrode surface during the different intercalation stages is still not completely clear. We combine different microscopy techniques including optical, scanning electron and electrochemical atomic force microscopies to analyze the morphological evolution of the graphite surface at different length scales as a function of the applied electrochemical potential. Whereas both carbon dissolution and blisters affect the surface on the micrometer scale as soon as intercalation starts, we find that the graphite surface is cracked on the sub-millimeter scale only when intercalation at a higher potential is reached, inducing a significant aging of the electrode surface.

INTRODUCTION. Perchloric acid ($HClO_4$) has been traditionally exploited as the electrolyte for electrochemical graphite delamination[1]. Chlorate anions, surrounded by water molecules (solvated anions), percolate within the graphite crystal through defects on the surface and inside the stratified crystal. At relative high electrochemical (EC) potentials, oxidation occurs and is accompanied by the formation of gas (namely CO, CO_2, O_2), which swells the uppermost graphite layers and produces blisters on the electrode surface[2,3,4,5]. The presence of solvated anions in the graphite inter-layer spaces screens the layer-layer interaction favoring crystal delamination; the latter usually occurs after a gentle sonication[6], which results in an electrolyte containing small graphene flakes (lateral size of the order of several μm)[7]. Currently, this electrochemical protocol represents one of the cheapest ways to produce large amounts of

graphene sheets. Consequently, there is a strong interest in its further optimization, *i.e*. in maximizing the number of single graphene flakes, reducing the number of defects as well as the production costs. The main research direction involves the use of different electrolytes, which can fulfill the above requirements[6,7,8]. Another strategy exploits standard diluted oxoacids as electrolytes, tuning the chemical and/or EC conditions[9,10,11,12]. In this respect, the morphological and structural evolution of the pristine graphite crystal, after the immersion in the EC cell at different EC potentials, plays a key role to understand intercalation and delamination processes. Following this idea, we have recently studied the early stages of anion intercalation in a highly oriented pyrolytic graphite (HOPG) crystal by EC scanning tunneling and atomic force microscopy (EC-STM and EC-AFM, respectively)[10]. These techniques enable to follow the changes of the graphite basal plane directly inside the EC cell[10,11]. Cyclic voltammetry (CV)[10] or normal pulse voltammetry (NPV)[12] have been exploited to activate the intercalation processes (CV)[10] and/or induce specific reactions on the graphite surface (NPV)[12]. Very recently, $HClO_4$ has been used to produce graphite oxide with a fine control in the oxidation level[13] or to dissolve a carbon-based material and obtain a high carbon concentration solution[14]. Such results need a further investigation in view of a better control of the HOPG evolution in acid environments under EC conditions.

To this goal, here we present and discuss a detailed microscopic investigation of HOPG immersed in $HClO_4$ not only focused on the early intercalation stages [at 0.95 V *vs*. a Pt quasi-reference (PtQRef)][10], but extended towards the oxygen evolution reaction at high EC potentials (namely 1.3 V *vs.* PtQRef). The CV demonstrates a clear evolution as a function of the EC potential but a corresponding morphological characterization of the electrode surface is still missing. By combining an investigation by *in-situ* optical microscopy and EC-AFM together

with a scanning electron microscopy (SEM), we succeeded in following the surface changes at different length scales (from millimeters down to a few micrometers). We observe carbon dissolution, blisters and fractures formation, which represent a progressive detriment for the crystal as higher EC potentials are applied. The surface chemistry was monitored by Raman spectroscopy focusing, in particular, on the electrode cracks appearing on the surface when the EC potential reaches 1.0 V vs PtQRef.

MATERIALS AND METHODS. A diluted (2 M) $HClO_4$ (Sigma-Aldrich S.R.L.) electrolyte was prepared and purified by argon bubbling in a separate flask for several hours. A z-grade HOPG (Optigraph GmbH) (20 × 10 × 1) mm^3 was exfoliated by an adhesive tape along the 20 mm edge and used as working electrode (WE) in a three-electrodes cell. A 0.5 mm-thick Pt wire was placed along the wall of the cell and used as a counter electrode (CE). A Pt wire was also exploited as a quasi-reference electrode (PtQRef)[15,16]. The latter possesses a stability down to a few mV and a well-characterized energy shift with respect to the standard hydrogen electrode (ΔV = 0.743 mV). A 5500 Keysight Technology EC-AFM was used in contact mode for the sample analysis *in-situ*. A CCD camera allows for the tip alignment on the immersed sample and was exploited to acquire *in-situ* images on the sub-mm scale. An Olympus BX41 optical microscope was used to characterize different areas of the sample after the intercalation process. The sample was removed from the EC cell, dried with nitrogen and placed below the microscope objective. The same protocol was used before acquiring the SEM images with a ZEISS Supra 40 field emission SEM, using an in-lens detector for secondary electrons; a very low accelerating voltage (800 V) and a very short working distance (less than 3 mm) were employed in order to avoid electron beam-induced surface damage while maintaining a good resolution. Finally, Raman spectra were recorded with a Jobin Yvon Labram HR800 Raman spectrometer coupled

with an Olympus BX41 microscope. Spectra were acquired in backscattering geometry (averaging 4 acquisitions of 60 s each) using a 50× objective. The 632.8 nm excitation laser line(He-Ne), focused on a spot of approximately 3 μm^2, was kept at 0.5 mW to prevent possible photo and/or thermal degradation of the samples.

RESULTS AND DISCUSSION. **Figure 1** demonstrates four voltammograms representative of the different intercalation stages of HOPG in 2 M $HClO_4$.

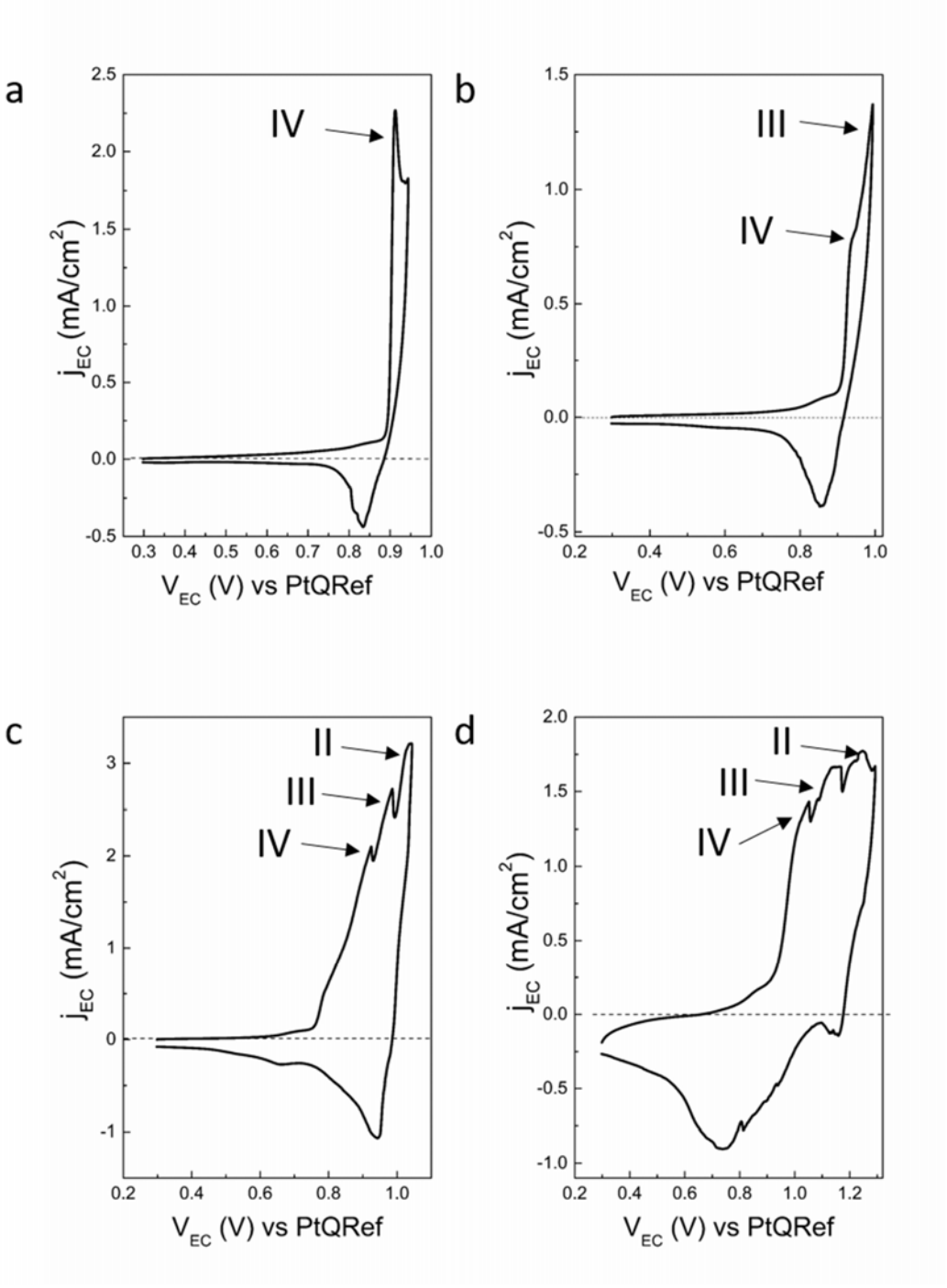

Figure 1. Cyclic voltammetry of HOPG in diluted (2 M) $HClO_4$ electrolyte (v_{scan} = 25 mV/s). a) first scan up to 0.95 V; the IV intercalation stage is labeled. b) second scan up to 1.0 V; the III intercalation stage appears. c) third scan up to 1.05 V, where the II intercalation stage is labeled. d) since the fourth scan, the CV shows the same voltammogram up to 1.3 V.

The different peaks are attributed to various intercalation stages (IV, III and II), as reported in the literature[17]. When the N^{th}-stage (here, IV, III or II) is reached, the solvated anions layers are statistically separated by (N-1) graphite layers[3,4,17]. With 2 M perchloric electrolyte, the II stage is the last one, because the final intercalation stage (I) requires such a large potential that side reactions take place instead[17]. The 2 M acid concentration is usually chosen in EC-SPM investigations since, on the one hand, it ensures a good anion intercalation and, on the other hand, it avoids a complete graphite dissolution, which would prevent data acquisition.

We observe that during the different cycles (panels *a* to *d* in Fig. 1) the ratio between the areas subtended below the anodic (positive) and cathodic (negative) peaks (*i.e*. the ratio between the anodic and cathodic exchanged charges) is close to 1, suggesting that the EC process is quasi-reversible, as reported in the literature[1,17].

Optical microscopy analysis. In a potential range where no Faradaic currents flow through the sample, the graphite basal plane is morphologically stable in the electrolyte solution (see **Figure 2***a*). At EC potentials below the III intercalation stage, the surface of the electrode remains unaffected (panel *b*). Conversely, its morphology significantly changes when the stage III is reached. At this stage, we observe the formation of a textured surface with ‘cracks’ on the electrode, homogenously affecting the whole surface (panel *c*).

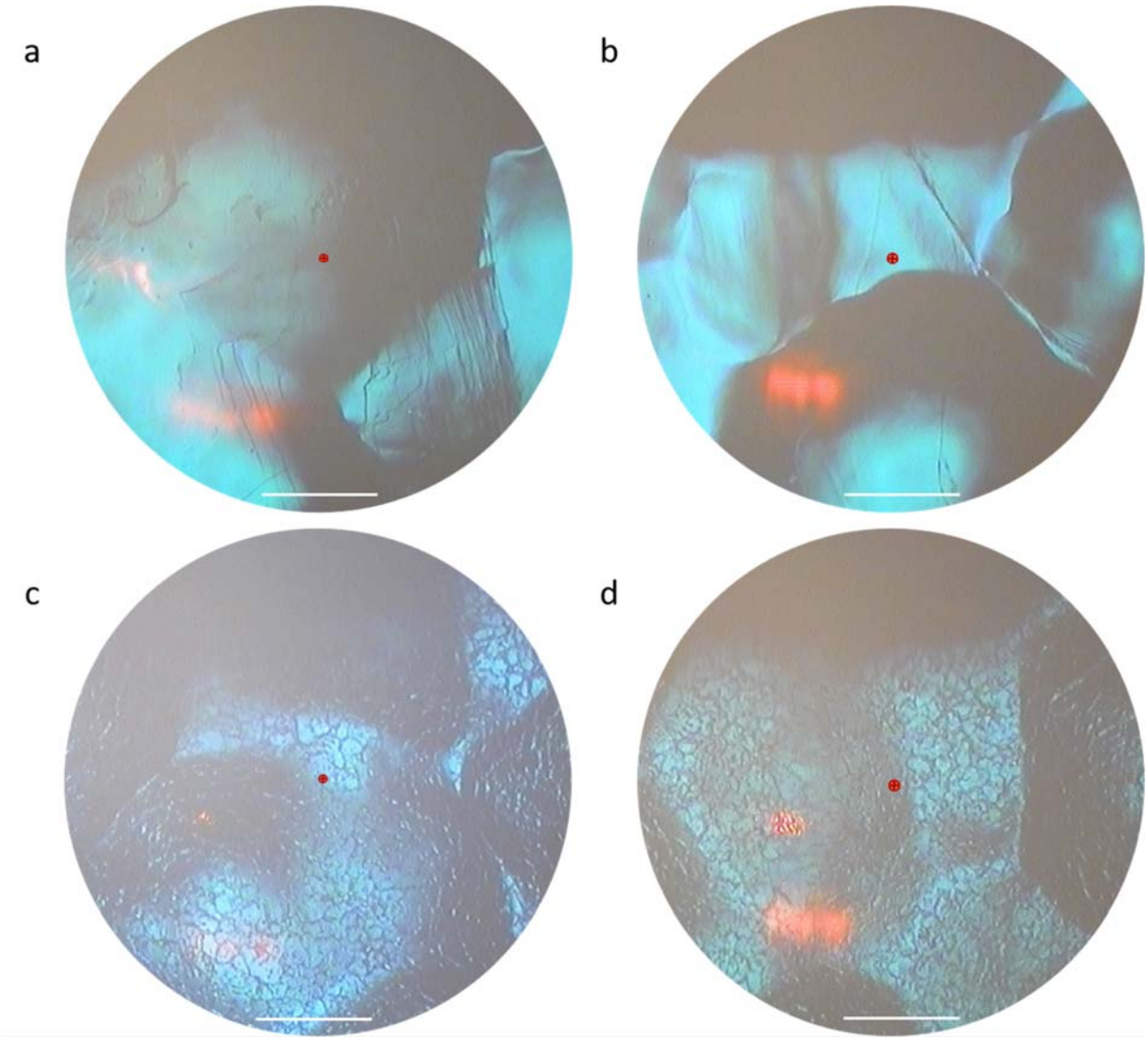

Figure 2. *In-situ* optical microscopy images acquired at different intercalation stages. Scale bar = 200 μm. a) unperturbed basal plane at 0.75 V. b) After a cyclic voltammetry up to 0.95 V (IV intercalation stage). c) After a cyclic voltammetry up to 1.0 V (III intercalation stage). Surface cracks are visible in the image. d) After a cyclic voltammetry up to 1.05 V (II intercalation stage). In these conditions, cracks continue to affect the electrode surface.

No further significant surface modifications are recorded at larger EC potentials (Fig. 2*d*). The surface morphology of the electrode is stable also when the electrode is extracted from the cell. **Figure 3** shows an image acquired in air with a higher magnification.

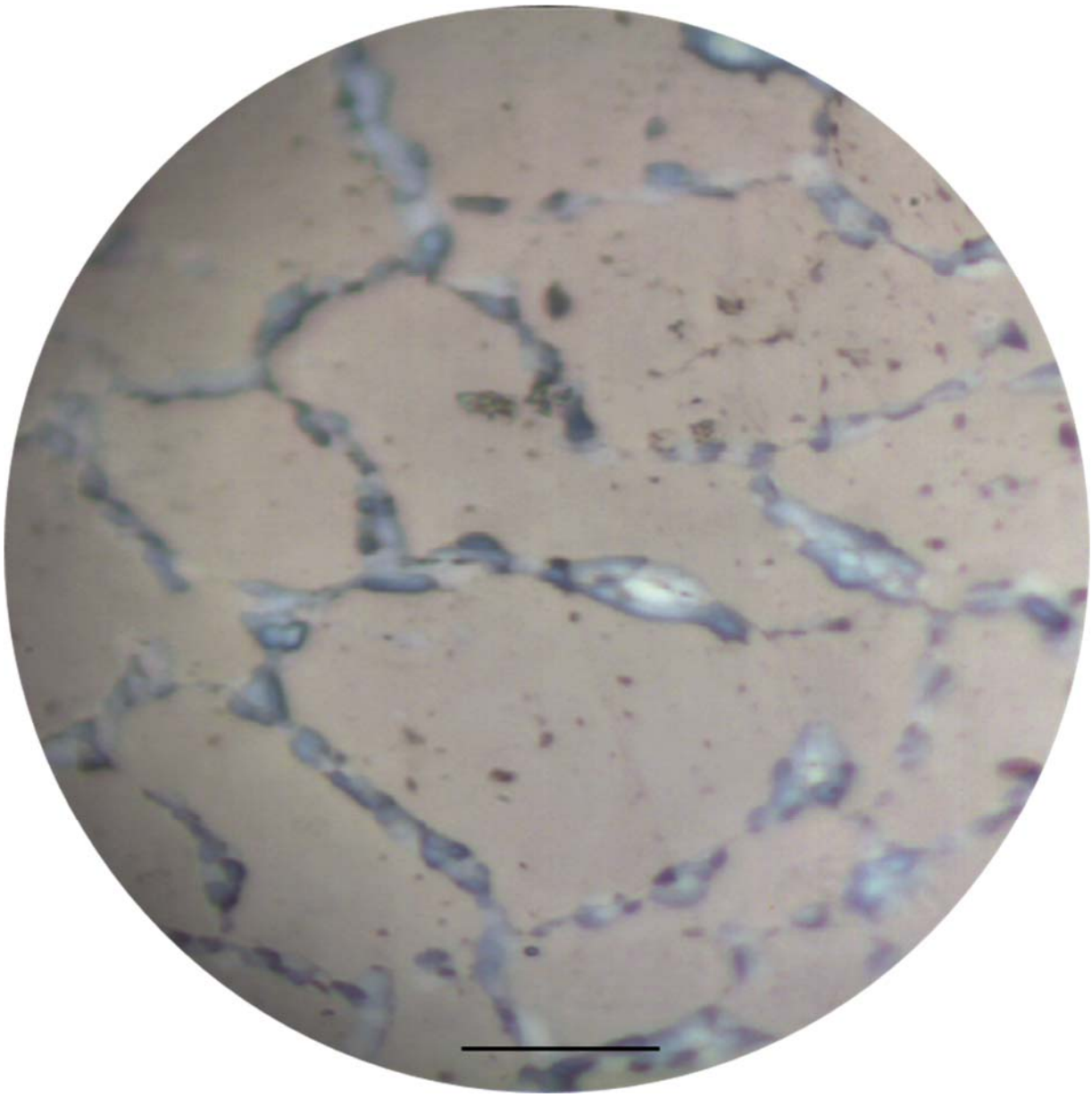

Figure 3. Optical microscopy image acquired after the III intercalation stage. Surface cracks appear bright, due to the diffusion of white light used to shine the samples. Scale bar = 15 μm.

Scanning Electron Microscopy (SEM) analysis. After the extraction of the sample from the EC cell, Scanning Electron Microscopy has been performed in order to assess the nature of the features described above and to acquire high-resolution images of the graphite surface at an intermediate

spatial scale between that of the optical microscopy analysis (from a few micrometers up to millimeters) and that of Atomic Force Microscopy (down to the nanometer scale, see below).

Figures 4 and **5** show images at different magnification of a graphite electrode surface after EC cycles up to 1 V or 1.1 V (*i.e.*, after reaching the III intercalation stage, like the conditions of the sample analyzed in Figs. 2-3). Different features can be observed:

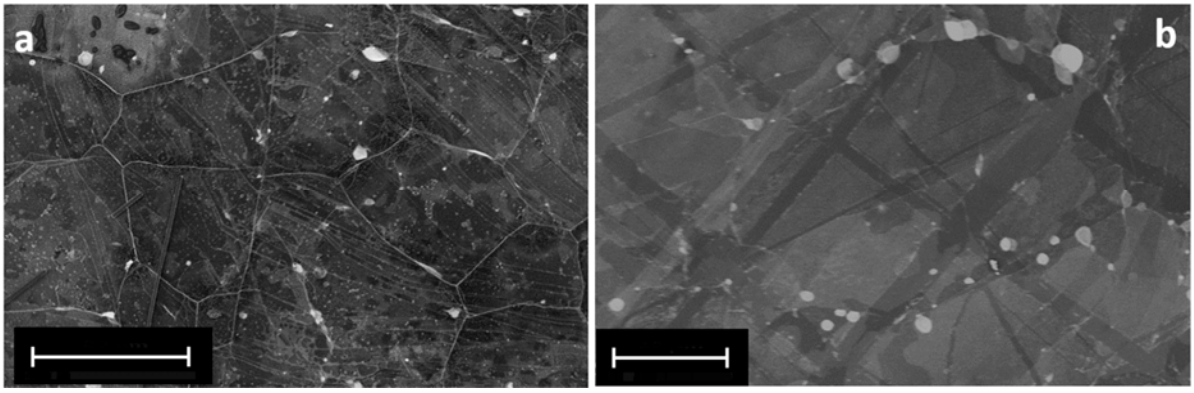

Figure 4. SEM images of the graphite surface after the III intercalation stage. a) scale bar = 20 μm; b) scale bar = 10 μm.

- At a smaller magnification (Fig.4) the surface is characterized by the presence of 'tiles' (with typical linear size of the order of tens of μm) separated by cracks or fractures, which reasonably correspond to those observed by optical microscopy (Fig. 2*c* or *d* and Fig. 3). These cracks are often decorated with brighter spots (Fig. 4*b*), which we identify as blisters. We note that such a surface cracking is not observed when the graphite surface is in the cell without any applied EC potential (not shown).
- At a larger magnification (Fig. 5) the surface presents straight parallel 'lines' (red arrows in Fig. 5) corresponding to the steps of the graphite surface, together with irregular, randomly oriented 'cracks'. The interpretation of the cracks as surface fractures is now corroborated, together with the observation of the blister decoration (white arrow in Fig. 5*b*).

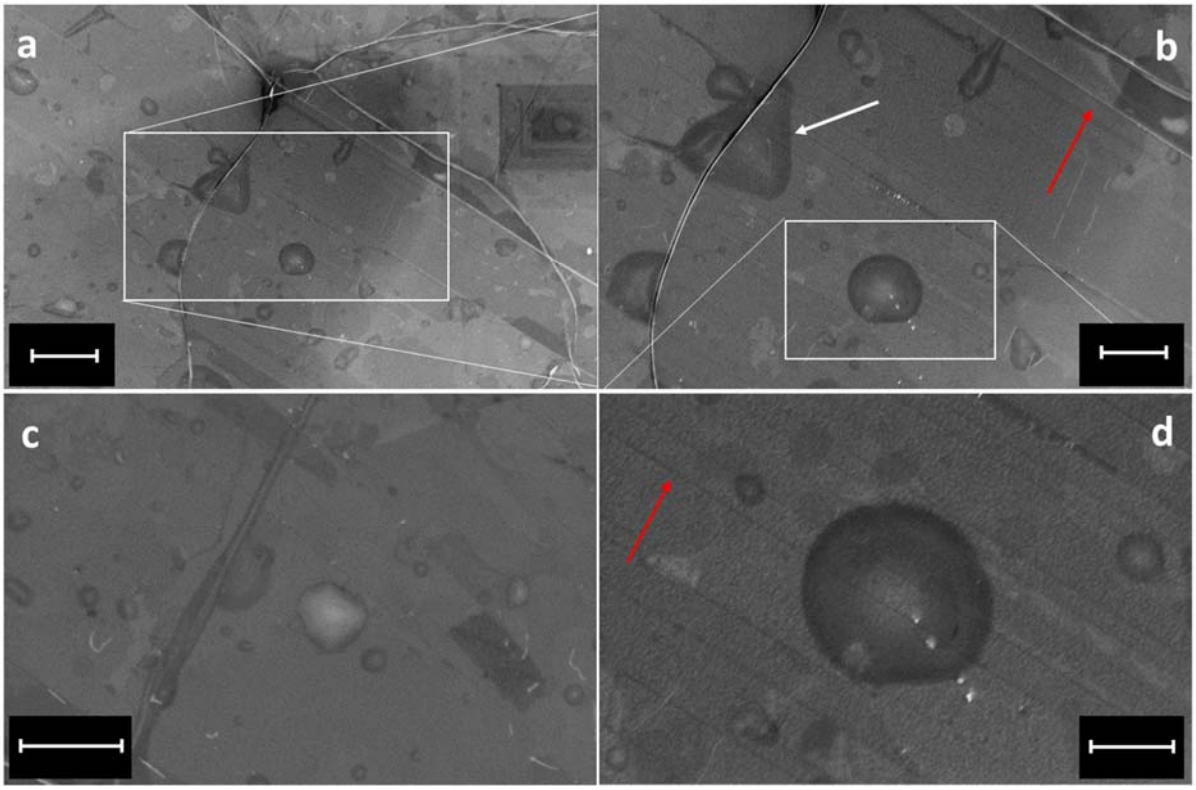

Figure 5. SEM images of the graphite surface after the III intercalation stage; panels a) (scale bar = 4 μm), b) (scale bar = 2 μm) and d) (scale bar = 1 μm) represent details of the same surface region at different magnifications. Panel c) represents a different region of the surface (scale bar = 2 μm).

- A closer inspection of the blisters enables their identification as 'bubbles', which seem to be protruding from the underlying surface (Fig. 5*d*). The typical size of these blisters is around few μm^2. Similar blisters have already been observed by AFM in our previous work[10] and will be analyzed in more detailed in the next section.
- Interestingly, most of the blisters are stable as it can be observed by acquiring images at different time intervals. Only those blisters that have been subjected to the SEM e-beam irradiation appear to have become unstable. As a matter of fact, they tend to disappear, or to 'deflate' (see **Figure 6***a* and 6*b*, taken on the same region a few minutes after each other), especially if a high acceleration voltage is applied. A possible interpretation is that the gases produced during the anion intercalation and entrapped inside the layered structure of graphite can escape through defects on the basal plane.

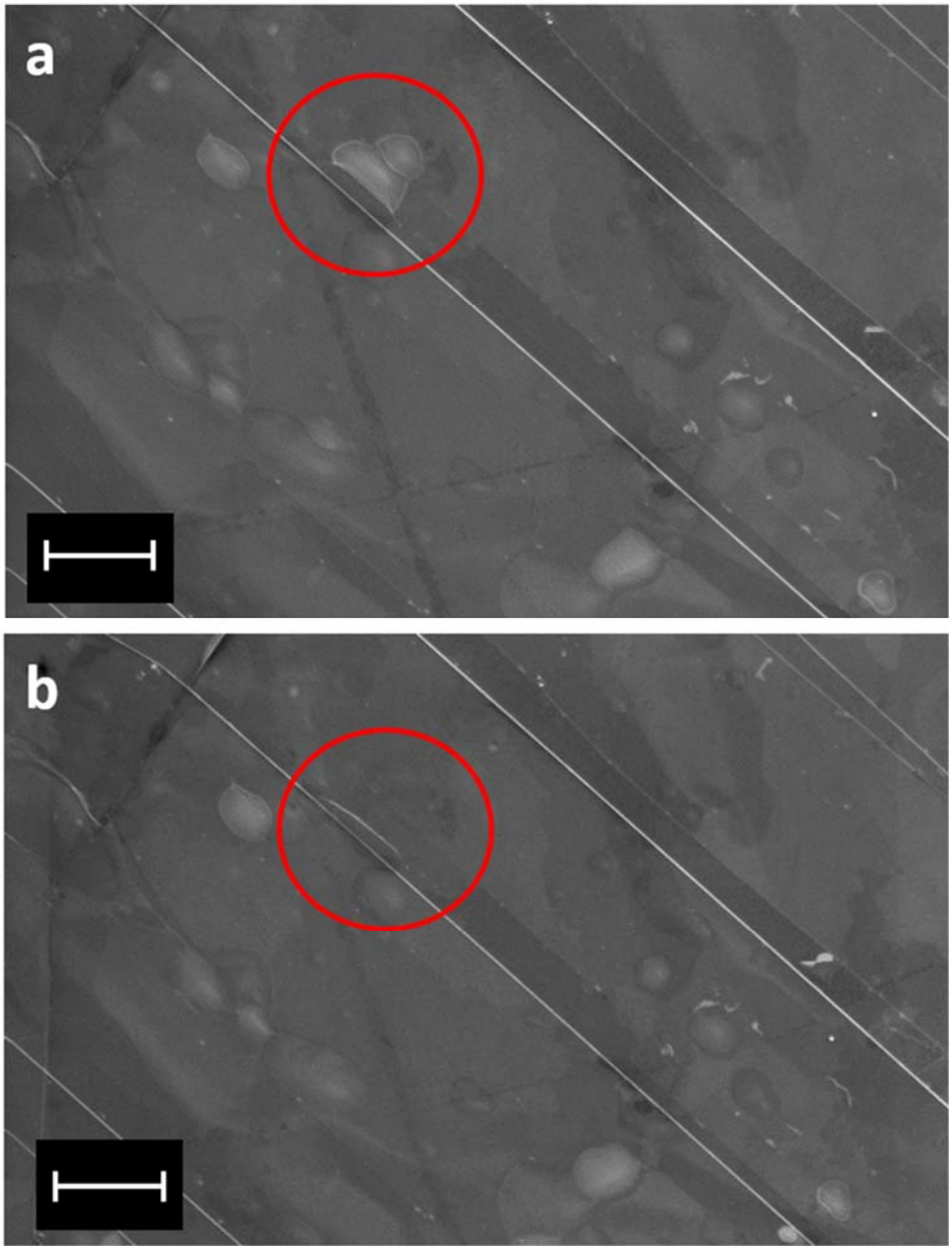

Figure 6. SEM images of the graphite surface after the III intercalation stage; panels a) and b) represent the same surface region (acquired about 1 min later with respect to the previous panel) before and after the 'disappearance' of a blister. Scale bars = 2 μm.

Raman spectroscopy analysis. In **Figures 7** and **8** we report the Raman spectra of a graphite electrode after a cyclic voltammetry up to the III intercalation stage compared with the Raman spectrum of the pristine (uncycled) HOPG electrode. The spectra were acquired focusing on the uniform region (tile), on a fracture line, and outside the electrochemically cycled region.

The absence of the D line (ascribed to presence of disorder[18,19,20] – *i.e.*, structural/chemical modifications of the graphite layers) indicates that the EC treatment produces surface blistering with no associated damage of the graphene layers at the nanometer scale. This is in agreement with the structural analysis of the blisters, which shows that the graphite lattice is largely preserved[10].

The main feature observed in the spectra of the cycled sample is the well-resolved doublet in the G line region at ~ 1600 cm^{-1}, which agrees with the literature on graphite intercalated compounds[21,22]. In our cycled sample (Fig. 8) we observe two sharp and well resolved components at 1587 cm^{-1} (G) and 1608 cm^{-1} (G', intercalation marker). Interestingly, after the intercalation processes associated with the electrochemical treatment, the D band (1250 – 1350 cm^{-1}) does not appear, while the 2D feature in the second order region (2400-2800 cm^{-1}) shows an overall reduced intensity with respect to pristine HOPG (Fig. 8).

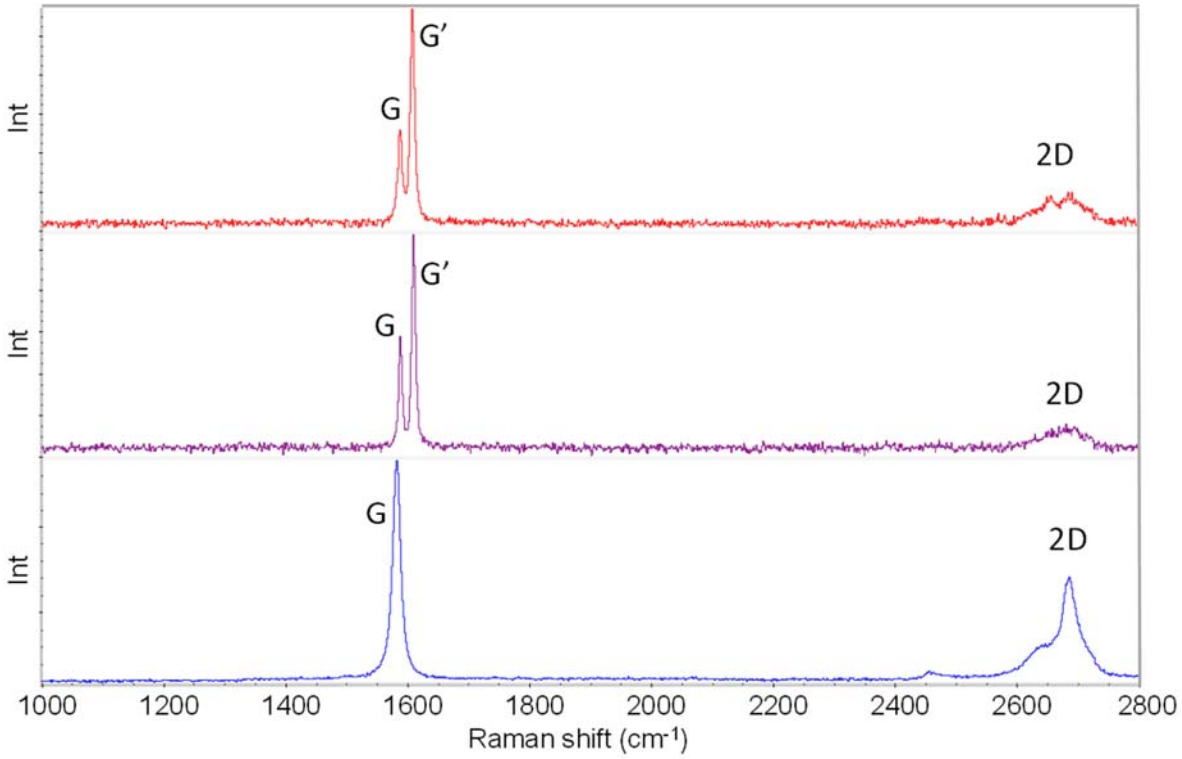

Figure 7. Raman spectra recorded at 632.8 nm in the range 1000 – 2800 cm^{-1}, after reaching the III intercalation stage during the CV. Red line: fracture; purple line: tile, blue line: pristine HOPG.

Since the G' line is observed after the EC treatment, we infer that a residual anion intercalation remains. Following refs. 21 and 22, the occurrence of the G-G' doublet is related to the presence of graphene layers in different local environments. The G line originates from stacks of graphene layers, while the G' line originates from graphene layers directly interacting with the anion intercalation layers[21,22]. This interaction leads to charge transfer on the graphene layers, which affects its electronic and vibrational structure, thus leading to the appearance of G'. This evidence is compatible with the structure of intercalation stages IV, III and II, where there are graphene planes both in contact with a layer of anions (G' line) and stacked graphene planes (G line).

The G' line of the fractured region slightly shifts towards lower wavenumbers with respect to that observed for the tile. This indicates a slightly different structure of the intercalated material in the region close to the fracture.

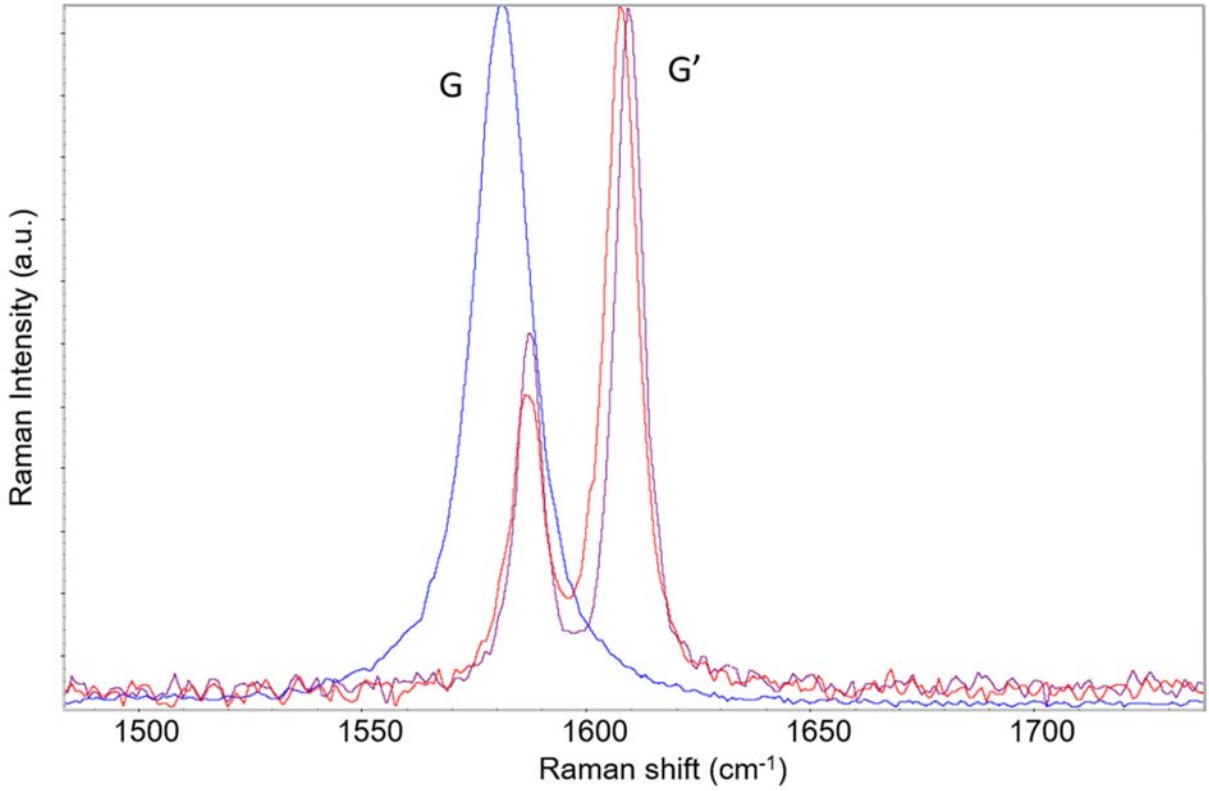

Figure 8. Raman spectra recorded at 632.8 nm in the range 1475 – 1750 cm^{-1}. Red line: fracture; purple line: tile, blue line: pristine HOPG. Enlargement of the G-G' region.

Another peculiar feature of the spectra obtained on the cycled material is the remarkable sharpening of the G line, with a FWHM that is almost half of the one in the pristine HOPG case. A sharpening of the G lines is reported for doped few-layer graphene[23] and has been related to a

change in the electronic structure of the doped layers, resulting in a shift of the Fermi energy level (E_F). This is consistent with the charge transfer effect discussed above. Similar effects on the shape of the G line in metallic and semiconducting nanotubes, ascribed to the modulation of the electronic structure, are also discussed in ref. 24.

EC-Atomic Force Microscopy (EC-AFM) analysis. AFM is used for an *in-situ* morphological characterization of the electrode surface. **Figure 9** reports the graphite evolution at different EC potentials. Below 0.95 V (panel *a*), the image confirms that the immersed sample is stable inside the electrolyte at the (sub-)micrometer scale. Figure 9*a* demonstrates the presence of flat terraces and sharp step edges, which appear to be stable as a function of time suggesting a negligible carbon dissolution at these applied potentials. Blisters appear in the acquired image (panel *b*) as soon as the IV intercalation stage is reached (at 0.95 V). These structures have an average lateral size of the order of 1 μm with a height in the 15-20 nm range.

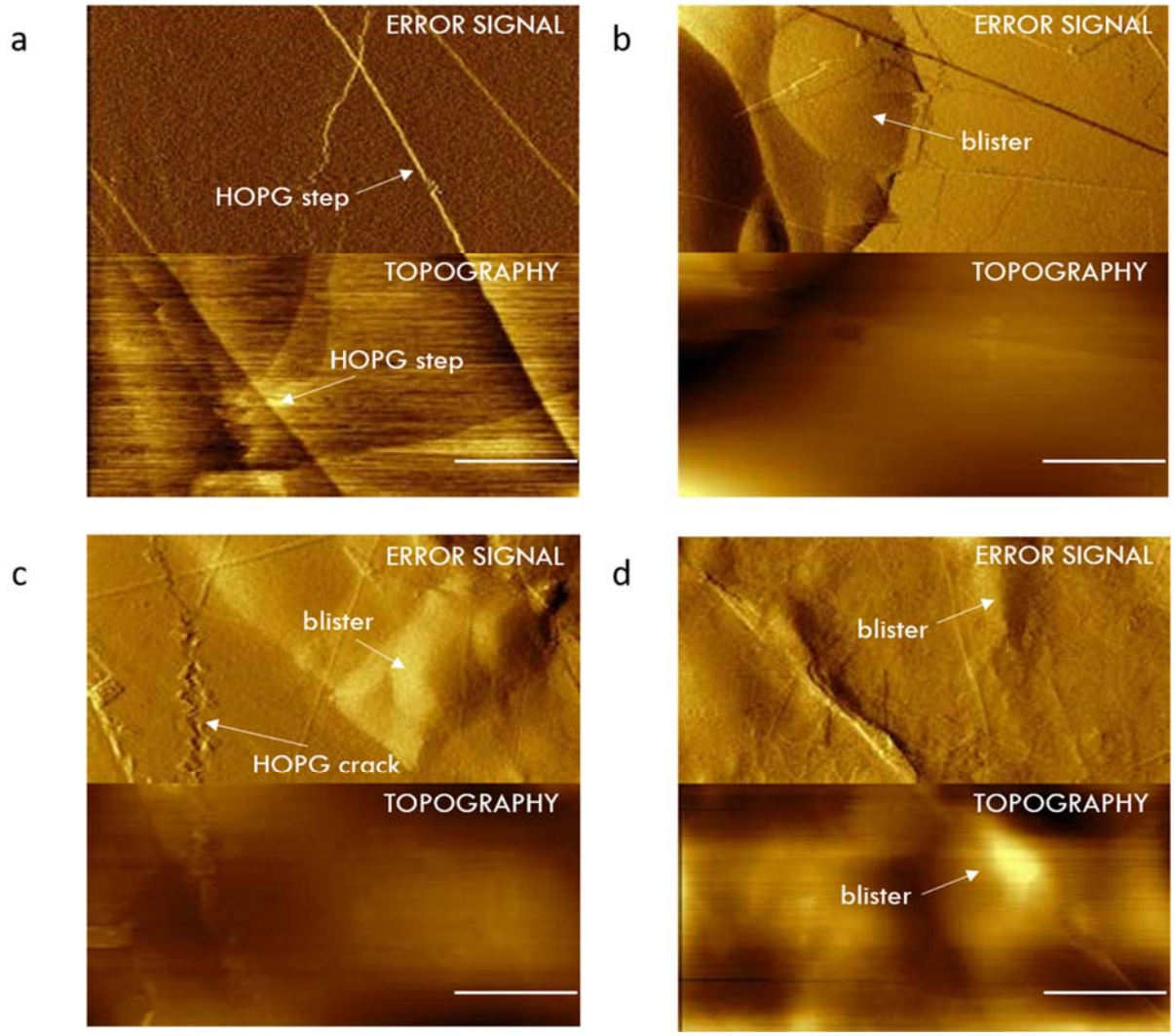

Figure 9. *In-situ* EC-AFM acquired at different intercalation stages. a) unperturbed basal plane at 0.75 V. b) after a CV up to 0.95 V (IV intercalation stage). Blisters are observed affecting the electrode surface. c) after a CV up to 1.0 V (III intercalation stage). d) after a CV up to 1.05 V (II intercalation stage). For all images: ERROR SIGNAL (down) vs TOPOGRAPHY (up), scale bar = 1 μm.

When the CV potential reaches 1.0 V (III intercalation stage, panel *c*), damages of the electrode surface are evident. The evolution of the blisters is accompanied by carbon dissolution affecting the graphite electrode at such high EC potentials[10,12]. Interestingly, we observe new zig-zag features formed along or close to the step edges (see the HOPG crack in the figure). These

fractures seem to be an armchair crack with additional branching that probably evolves along grain boundaries, monoatomic steps and defects[25]. At even higher applied potentials (see Figure 4*d*), the surface appears more eroded and affected by many wrinkles, to the detriment of the electrode.

EC-AFM offers the possibility to study the evolution of the electrode crack as a function of time (**Figure 10)**. The sample was cycled up to the III intercalation stage (1.0 V) and then kept at 0.3 V, during the EC-AFM acquisition (panels from *a* to *g*). The fracture propagation evolves in some minutes, probably assisted by the carbon dissolution favored by the electrolyte solution[26].

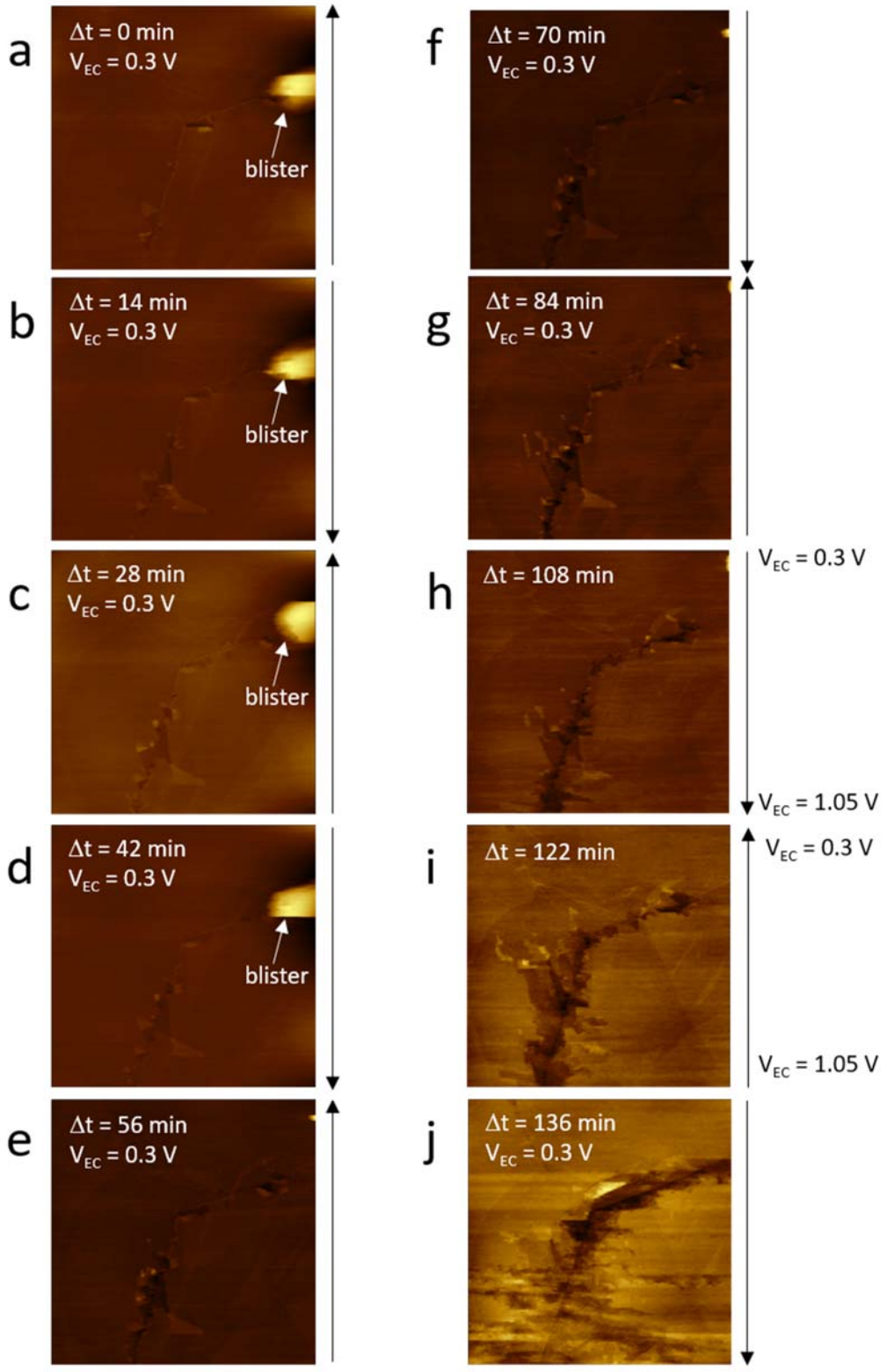
a
Δt = 0 min
V_{EC} = 0.3 V
blister
b
Δt = 14 min
V_{EC} = 0.3 V
blister
c
Δt = 28 min
V_{EC} = 0.3 V
blister
d
Δt = 42 min
V_{EC} = 0.3 V
blister
e
Δt = 56 min
V_{EC} = 0.3 V
f
Δt = 70 min
V_{EC} = 0.3 V
g
Δt = 84 min
V_{EC} = 0.3 V
h
Δt = 108 min
V_{EC} = 0.3 V
V_{EC} = 1.05 V
i
Δt = 122 min
V_{EC} = 0.3 V
V_{EC} = 1.05 V
j
Δt = 136 min
V_{EC} = 0.3 V

Figure 10. *In-situ* EC-AFM 4 x 4 μm^2 acquired after a CV extended up to the III intercalation stage (1.0 V). Panels from a) to g) are acquired in sequence. The interval (Δt) reported in each image refers to the time delay in the image acquisition with respect to the image of panel a). h) and i) EC-AFM acquisition is synchronized with a CV up to the III intercalation stage. j) image acquired at a EC potential of 0.3 V after the CV. The arrows on the right side of the images show the scanning direction.

Blisters are known to evolve due to the development of CO, CO_2 and O_2[1,2,3,4] produced during the oxidation of the graphite. In panels *a-d*, a blister is clearly visible and it remains stable in the same position for ~45 minutes. In panel *e*, the abrupt disappearance of the blister can be interpreted in terms of the removal of gas through a microscopic vent, in analogy with the reported SEM analysis (see Fig. 6). After the blister deflation, the EC-AFM image reveals flat terraces in which only fractures and erosions are visible. This suggests that HOPG undergoes an elastic deformation during the surface blistering. In panels *h* and *i*, the EC potential is synchronized with the microscopy acquisition. This means that each AFM scan line is acquired at a different potential, as indicated. Interestingly, we note that the carbon dissolution is very fast along the fracture, while terraces are much more stable. In panel *j*, we observe that despite the EC potential is again set at 0.3 V (a value where the HOPG basal plane is largely stable) the carbon dissolution continues and graphite seems to be dissolved by the electrolyte. After further 30 minutes at 0.3 V, the dissolution process is spontaneously blocked and can be activated only when the EC potential is tuned again to the III intercalation stage (not shown).

CONCLUSIONS. The increasing request in the optimization of chemical graphene production pushes towards a better comprehension of the molecular mechanisms involved in the graphite delamination process. A renewed interest has been reported in the electrochemical strategies for the production of graphene, where the intercalation of anions inside the graphite electrode is followed by a delamination of the crystal. Researchers have focused their studies on oxoacid electrolytes used for intercalation[9,10,11,12]. Among them, the effects on the quality of the electrode

surface morphology when diluted perchloric solutions are used at different EC potentials are still partially unknown. For this reason, we combined different microscopic and spectroscopic techniques to observe the electrode evolution at different intercalation anion stages. We find that the graphite basal plane maintains good elastic properties even after the surface deformation induced by blisters occurs. On the contrary, as soon as the III intercalation stage is reached surface cracks are observed, caused by the heavy carbon dissolution process acting at these potentials. Even when the graphite potential is turned back to that of the IV intercalation stage or below, the electrode detriment continues for about half an hour starting from the crack edges and continuing towards the HOPG terraces.

ACKNOWLEDGMENT.

The authors declare no financial support. We are grateful to P. Biagioni (Department of Physics, Politecnico di Milano) for useful discussion. This work was achieved at the Solid-Liquid Interface and Nanomicroscopy (SoLINano) laboratory, which is an inter-Departmental laboratory of the Politecnico di Milano.

REFERENCES.

1) Kinoshita, K. *Carbon. Electrochemical and Physicochemical Properties*. John Wiley & Sons: New York, 1988.
2) Dresselhaus, M. S.; Endo, M. In *Graphite Intercalation Compounds II*; Zabel, H., Solin, S. A. Eds.; Springer-Verlag: Berlin Heidelberg, 1992; pp 347-441.
3) Beck, F.; Krohn, H. Reversible Electrochemical Intercalation of Anions from Aqueous Solutions in Polymer Bound Graphite Electrodes. *Synth. Met*. **1983**, *7*, 193-199.

4) Goss, C. A.; Brumfield, J. C.; Irene, E. A.; Murray, R. W. Imaging the Incipient Electrochemical Oxidation of Highly Oriented Pyrolytic Graphite. *Anal. Chem.* **1993**, *65*, 1378-1389.

5) Hathcock, K. W.; Brumfield, J. C.; Goss, C. A.; Irene, E. A.; Murray, R. W. Incipient Electrochemical Oxidation of Highly Oriented Pyrolytic Graphite: Correlation between Surface Blistering and Electrolyte Anion Intercalation. *Anal. Chem*. **1995**, *67*, 2201-2206.

6) Nicolosi, V.; Chhowalla, M.; Kanatzidis, M. G.; Strano, M. S.; Coleman, J. N. Liquid Exfoliation of Layered Materials. *Science* **2013**, *340*, No. 1226419.

7) Catheline, A.; Ortolani, L.; Morandi, V.; Melle-Franco, M.; Drummond, C.; Zakri, C.; Pénicaud, A. Solutions of Fully exfoliated Individual Graphene Flakes in Low Boiling Point Solvents. *Soft Matter*. **2012**, *8*, 7882-7887.

8) An, H.; Tan, B. H.; Moo, J. G. S.; Liu, S.; Pumera, M.; Ohl, C.-D. Graphene Nanobubbles Produced by Water Splitting. *Nano Lett*. **2017**, *17*, 2833-2838.

9) Xia, Z. Y.; Pezzini, S.; Treossi, E.; Giambastiani, G.; Corticelli, F.; Morandi, V.; Zanelli, A.; Bellani, V.; Palermo, V. The Exfoliation of Graphne in Liquids by Electrochemical, Chemical and Sonication-Assisted Techniques: a Nanoscale Study. *Adv. Funct. Mater*. **2013**, *23*, 4684-4693.

10) Bussetti, G.; Yivlialin, R.; Alliata, D.; Li Bassi, A.; Castiglioni, C.; Tommasini, M.; Casari, C. S.; Passoni, M.; Biagioni, P.; Ciccacci, F.; et al. Disclosing the Early Stages of Electrochemical Anion Intercalation in Graphite by a Combined Atomic Force Microscopy/Scanning Tunneling Microscopy Approach. *J. Phys. Chem. C* **2016**, *120*, 6088-6093.

11) Yivlialin, R.; Brambilla, L.; Bussetti, G.; Tommasini, M.; Li Bassi, A.; Casari, C. S.; Passoni, M.; Ciccacci, F.; Duò, L.; Castiglioni, C. Evolution of the Graphite Surface in Phosphoric Acid: an AFM and Raman Study. *Beilstein J. Nanotechnol*. **2016**, *7*, 1878-1884.

12) Yivlialin, R.; Bussetti, G.; Magagnin, L.; Ciccacci, F.; Duò, L. Temporal Analysis of the Blister Evolution during Anion Intercalation in Graphite. *Phys. Chem. Chem. Phys.* **2017**, *19*, 13855-13859

13) Tian, Z.; Yu, P.; Lowe, S. E.; Pandolfo, A. G.; Gengenbach, T. R.; Nairn, K. M.; Song, J.; Wang, X.; Zhong, Y. L.; Li, D. Facile Electrochemical Approach for the Production of Graphite Oxide with Tunable Chemistry. *Carbon* **2017**, *112*, 185-191.

14) US patent: US 9,534,319 B2

15) Kasem, K. K.; Jones, S. Platinum as a Reference Electrode in Electrochemical Measurements. *Platinum Metals Rev*. **2008**, *52*, 100-106.

16) Inzelt, G. Pseudo-Reference Electrodes. Springer (2013).

17) Alliata, D.; Kötz, R.; Haas, O.; Siegenthaler, H. In Situ AFM Study of Interlayer Spacing during Anion Intercalation into HOPG in Aqueous Electrolyte. *Langmuir* **1999**, *15*, 8483-8489.

18) Ferrari, A. C.; Basko, D. M. Raman Spectroscopy as a Versatile Tool for Studying the Properties of Graphene. *Nature Nanotechnol*. **2013**, *8*, 235-246.

19) *Raman Spectroscopy in Graphene Related System*; Jorio, A., Dresselhaus, M. S., Saito, R., Dresselhaus, G., Eds.; Wiley-VCH Verlag: New York, 2011.

20) Castiglioni, C.; Tommasini, M.; Zerbi, G. Raman Spectroscopy of Polyconjugated Molecules and Materials: Confinement Effect in One and Two Dimensions. *Philos. Trans. R. Soc. Lond. Ser. A – Math. Phys. Eng. Sci*. **2004**, *362*, 2425-2459.

21) Alsmeyer, D. C.; McCreery, R. L. In Situ Raman Monitoring of Electrochemical Graphite Intercalation and Lattice Damage in Mild Aqueous Acids. *Anal. Chem*. **1992**, *64*, 1528-1533.

22) Dresselhaus, M. S.; Dresselhaus, G. Intercalation Compound of Graphite. *Adv. Phys*. **2002**, *51*, 1-86.

23) Bruna, M.; Borini, S. Observation of Raman G-Band Splitting in Top-Doped Few-Layer Graphene. *Phys. Rev. B* **2010**, *81* No. 125421.

24) Lazzeri, M.; Piscanec, S.; Mauri, F.; Ferrari, A. C.; Robertson, J. Phonon Linewidths and Electron-Phonon Coupling in Graphite and Nanotubes. *Phys. Rev. B* **2006**, *73*, No. 155426.

25) Xu, M.; Tabarraei, A.; Paci, J. T.; Oswald, J.; Belytschko, T. A Coupled Quantum/Continuum Mechanics Study of Graphene Fracture. *Int. J. Fract.* **2012**, *173*, 163-173.

26) Zhang, P.; Ma, L.; Fan, F.; Zeng, Z.; Peng, C.; Loya, P.E.; Liu, Z.; Gong, Y.; Zhang, J.; Zhang, X.; et al. Fracture Toughness of Graphene. *Nature Comm*. **2014**, *5*, No. 3782.